

4

Chapter 4

Impact of Suction or Blowing on Elastico-Viscous Hydromagnetic Fluid Flow Past a Stretching Permeable Sheet

4.1 Introduction

The stretching sheet problem in fluid dynamics find its place in industry because of it's numerous important applications. This type of problem often noticed in industry in manufacturing unit, such as rolling of artificial fibres, extraction of polymer sheet, glass-fibre production, crystal growing, paper production, crystal growing and so on.

Sakiadis [65] investigated the flow of boundary layer maintaing constant velocity past a moving rigid surface of it's own plane. The viscous boundary layer fluid flow past a linearly stretching sheet taking similarity transformation examined by Crane [66] analytically. Gupta *et al.* [67] has extended the heat transition and mass transport analysis of Crane's problem with suction or blowing effect. Parlov [68] presented the hydromagnetic viscous fluid past a plane deformed surface. Chakrabarti *et al.* [69] investigated the magnetohydrodynamic Newtonian fluid past a streatching sheet taking uniform temperature.

Crane's preliminary study further extended by research scientists like Vajravelu and Rollins [70], Chamkha [71], Zhang and Wang [72], Khan and Pop [73], Mahmoud [74], Hayat *et al.* [75], Chauhan and Olkha [76], Mahapatra *et al.* [77] and Ishak *et al.* [78] taking fluids of different classes with different physical situations. The above-mentioned works are noteworthy because in each paper undeniable important properties of boundary layer and the heat transition because of motion of the sheet are explained. He [79-82] laid the mathematical foundation of HPM. His work inspired many researchers at later stage to solve coupled nonlinear differential equations involved in fluid dynamics problems with this method.

The present study aims to examine the boundary layer electrically conducting hydromagnetic steady elastico-viscous fluid flow along a stretching permeable sheet using Homotopy Perturbation method. Walters liquid (Model B') exhibits the elastico-viscous property in the fluid. To study the impact of elastico-viscous parameter, magnetics parameter, suction and blowing parameters in the flow field, the analytically computed results of velocity expression and shear stress are plotted to bring out physical insight of the problem.

4.2 Mathematical Formulation

The steady electrically conducting hydromagnetic elastico-viscous boundary layer fluid flow along a stretching permeable sheet is considered. Using usual boundary layer and MHD approximation, the fluid motion governed by:

$$\frac{\partial u}{\partial x} + \frac{\partial v}{\partial y} = 0 \quad (4.2.1)$$

$$u \frac{\partial u}{\partial x} + v \frac{\partial u}{\partial y} = \nu \frac{\partial^2 u}{\partial y^2} - \frac{k_0}{\rho} \left[u \frac{\partial^3 u}{\partial x \partial y^2} + v \frac{\partial^3 u}{\partial y^3} - \frac{\partial u}{\partial y} \frac{\partial^2 u}{\partial x \partial y} + \frac{\partial u}{\partial x} \frac{\partial^2 u}{\partial y^2} \right] - \frac{\sigma B_1^2}{\rho} u \quad (4.2.2)$$

The last term of equation (4.2.2) is the contribution of electromagnetic force termed as Lorentz force under MHD approximation.

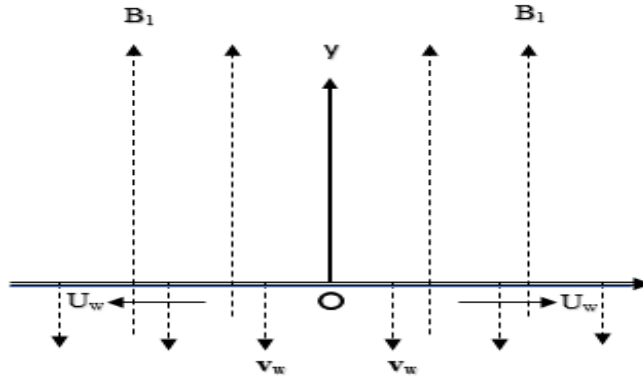


Fig. 4.1 Geometrical model of flow problem

The approximate boundary conditions are:

$$u = U_w = cx, \quad v = v_w \text{ at } y = 0; \quad u = 0 \text{ as } y \rightarrow \infty \quad (4.2.3)$$

where U_w is the stretching velocity, c is the stretching constant with $c > 0$. Here v_w is a specified distribution of suction ($v_w < 0$) or, blowing ($v_w > 0$).

Similarity solution of the above system of equations are:

$$u = cx f'(\eta), \quad v = -(cv)^{\frac{1}{2}} f(\eta) \quad (4.2.4)$$

where $\eta = y \left(\frac{c}{v}\right)^{\frac{1}{2}}$.

Using (4.2.4) in (4.2.2), the self-similar equations obtained as:

$$f''''(\eta) + f(\eta)f''(\eta) - [f'(\eta)]^2 - Mf'(\eta) - k_1[2f'(\eta)f'''(\eta) - [f''(\eta)]^2 - f(\eta)f''''(\eta)] = 0 \quad (4.2.5)$$

where $M = \frac{\sigma B_1}{c\rho}$ and $k_1 = \frac{k_0 c}{\rho v}$ are the modified magnetic and elasto-viscous parameter.

The boundary condition (4.2.3) reduces to

$$\text{At } \eta = 0, \quad f(\eta) = S, f'(\eta) = 1; \text{ as } \eta \rightarrow \infty f(\eta) = 0 \quad (4.2.6)$$

where $S = -\frac{v_w}{(cv)^{\frac{1}{2}}}$ represents suction for $v_w < 0$ and blowing for $v_w > 0$.

4.3 Method of Solution

Using Homotopy Perturbation Method, equation (4.2.5) is constructed as follows:

$$(1-p)(f'''' - Mf') + p[f'''' - Mf' + ff'' - f'^2 - k_1(2f'f''' - ff'''' - f''^2)] = 0 \quad (4.3.1)$$

We consider $f = f_0 + pf_1 + p^2f_2 + \dots$, and thus equation (4.3.1) becomes

$$\begin{aligned}
 (1-p)[(f_0'''' + pf_1'''' + p^2f_2'''' + \dots) - M(f_0' + pf_1' + p^2f_2' + \dots)] \\
 + p[(f_0'''' + pf_1'''' + p^2f_2'''' + \dots) - M(f_0' + pf_1' + p^2f_2' + \dots)] \\
 + (f_0 + pf_1 + p^2f_2 + \dots)(f_0'' + pf_1'' + p^2f_2'' + \dots) \\
 - (f_0' + pf_1' + p^2f_2' \dots)^2 - k_1\{2(f_0' + pf_1' + p^2f_2' + \dots)(f_0'''' \\
 + pf_1'''' + p^2f_2'''' + \dots) - (f_0 + pf_1 + p^2f_2 + \dots)(f_0^{iv} + pf_1^{iv} \\
 + p^2f_2^{iv} + \dots) - (f_0'' + pf_1'' + p^2f_2'' + \dots)^2\}] \\
 = 0
 \end{aligned} \tag{4.3.2}$$

Terms independence of p gives,

$$f_0'''' - Mf_0' = 0 \tag{4.3.3}$$

Transformed conditions at boundary are,

$$f_0(0) = S, f_0'(0) = 1, f_0'(\infty) = 0 \tag{4.3.4}$$

Term containing only p gives,

$$f_1'''' - Mf_1' = -f_0f_0'' - f_0'^2 + k_1(2f_0'f_0'''' - ff_0^{iv} - f_0'^2) \tag{4.3.5}$$

Transformed conditions at boundary are,

$$f_1(0) = 0, f_1'(0) = 0, f_1'(\infty) = 0 \tag{4.3.6}$$

Terms containing only p^2 gives,

$$\begin{aligned}
 f_2'''' - Mf_2' = -f_0f_1'' - f_1f_0'' + 2f_0'f_1' + k_1(2f_0'f_1'''' + f_1'f_0'''' - f_0f_1^{iv} - f_1f_0^{iv} \\
 - 2f_0''f_1'')
 \end{aligned} \tag{4.3.7}$$

Transformed conditions at boundary are,

$$f_2(0) = 0, f_2'(0) = 0, f_2'(\infty) = 0 \tag{4.3.8}$$

Solving equations (4.3.3), (4.3.5), and (4.3.7) with the help of boundary conditions (4.3.4), (4.3.6), and (4.3.8), we get

$$f_0 = A_1 + A_2e^{-\sqrt{M}\eta} \tag{4.3.9}$$

$$f_1 = D_8 + D_9 e^{-\sqrt{M}\eta} + K_2(D_5 e^{-2\sqrt{M}\eta} + D_6 e^{-\sqrt{M}\eta}) \tag{4.3.10}$$

$$f_2 = D_{33} + D_{34}e^{-\sqrt{M}\eta} + D_{28}e^{-2\sqrt{M}\eta} + K_2(D_{29}e^{-2\sqrt{M}\eta} + D_{30}e^{-2\sqrt{M}\eta} + D_{31}e^{-3\sqrt{M}\eta}) \quad (4.3.11)$$

Hence,

$$f(\eta) = A_1 + A_2e^{-\sqrt{M}\eta} + p[D_8 + D_9e^{-\sqrt{M}\eta} + K_2(D_5e^{-2\sqrt{M}\eta} + D_6e^{-\sqrt{M}\eta})] + p^2[D_{33} + D_{34}e^{-\sqrt{M}\eta} + D_{28}e^{-2\sqrt{M}\eta} + K_2(D_{29}e^{-2\sqrt{M}\eta} + D_{30}e^{-2\sqrt{M}\eta} + D_{31}e^{-3\sqrt{M}\eta})] + \dots \dots \dots \quad (4.3.12)$$

Differentiating equation (4.3.12) with respect to η , we obtain

$$f'(\eta) = D_{35}e^{-\sqrt{M}\eta} + p[D_{36}e^{-\sqrt{M}\eta} + K_2(D_{37}e^{-2\sqrt{M}\eta} + D_{38}e^{-\sqrt{M}\eta})] + p^2[D_{39}e^{-\sqrt{M}\eta} + D_{40}e^{-2\sqrt{M}\eta} + K_2(D_{41}e^{-2\sqrt{M}\eta} + D_{42}e^{-2\sqrt{M}\eta} + D_{43}e^{-3\sqrt{M}\eta})] + \dots \dots \dots \quad (4.3.13)$$

The constants of the above equations are obtained but not given here for the sake of brevity.

4.4 Results and Discussions

The expression for approximate skin friction coefficient is given by

The skin friction at the sheet is obtained as

$$\tau = f''(0) + k_1\{f(0)f'''(0) + 3f'(0)f''(0)\} \quad (4.4.1)$$

The numerical computations for the velocity component and skin friction at the sheet are obtained by analytic method. The Matlab software is used for computation and graphical representation to observed the effects of different flow parameters viz., visco-elastic parameter k_1 , magnetic parameter M and suction or blowing parameter S . The elasto-viscous effect is displayed by the parameter k_1 . Setting $k_1=0$, it is possible to obtain the results for Newtonian fluid.

Figure 4.2 illustrates the velocity distribution with variation of elasto-viscous parameter k_1 for $S = 0$ with $M = 4$, $p = 1$. With the rising magnitude of elasto-viscous parameter, the motion of the fluid diminishes and gradually vanishes with progressive

distance from the sheet. Further, it is noticed that velocity diminishing rate is higher for non-Newtonian case in comparison with Newtonian case.

The velocity distribution with variation of magnetic parameter is depicted in figure 4.3 for $S = 0$ with $k_1 = 0.1$, $p = 1$. With the growth of M , velocity reduces for fixed η . The magnetic field exerts Lorenz force which retards the fluid motion. With increasing distance, the velocity vanishes. The thickness reduces for boundary layer with the growth of M which can be found from velocity curves.

Figures 4.4 and 4.5 depict the velocity profile against η across the boundary layer for suction and blowing parameter variation for fixed values of $M = 4$, $k_1 = 0.1$ and $p = 1$. It has been observed that the velocity curves rise with the growth of applied suction but diminishes for the growth of blowing. Thus, blowing helps to diminish the thickness of boundary layer but suction shows opposite behaviors.

Figures 4.6 to 4.8 reveal the shearing stress at the stretching sheet against M and S for different values of k_1 . Figure 4.6 demonstrates that the shearing stress reduces initially for fixed values of M for elasto-viscosity growth. But it enhances with the rising magnitude of magnetic parameter $M = 4$ onwards. Figure 4.7 illustrates that the shearing stress enhances in the beginning as elastic-viscous parameter rises for fixed $M = 4$, $k_1 = 0.1$ and $p = 1$, but it reduces gradually as applied suction increases. Further, figure 8 displays that the shearing stress diminishes in the beginning with rising magnitude of elasto-viscous parameter for fixed $M = 4$, $k_1 = 0.1$ and $p = 1$ but it enhances gradually as applied blowing increases.

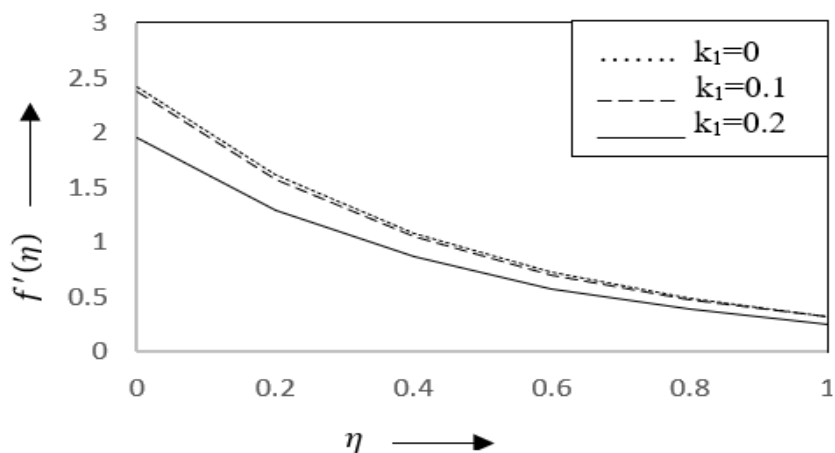


Fig. 4.2 Velocity profile $f'(\eta)$ against η for variation of k_1

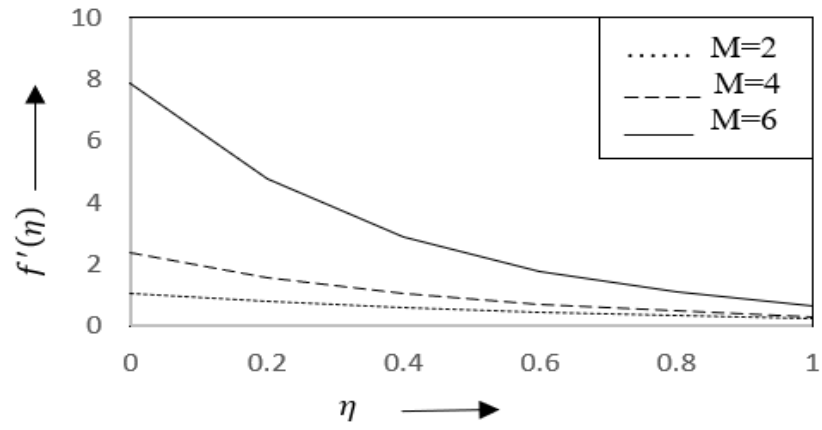


Fig. 4.3 Velocity profile $f'(\eta)$ against η for variation of M

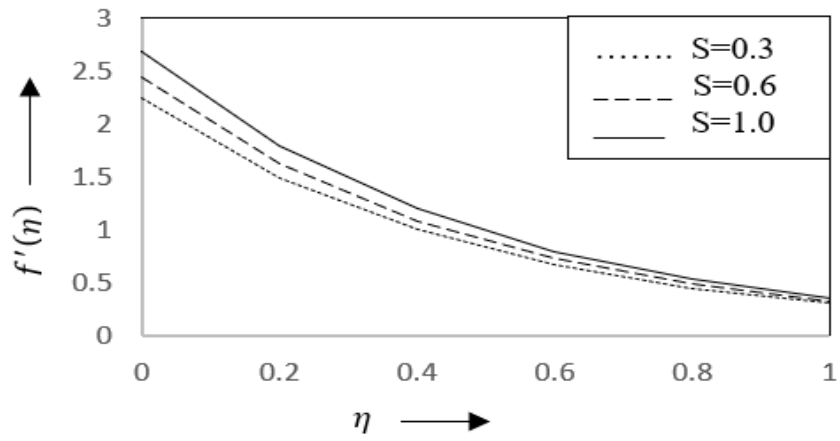


Fig. 4.4 Velocity profile $f'(\eta)$ against η for variation of S (suction)

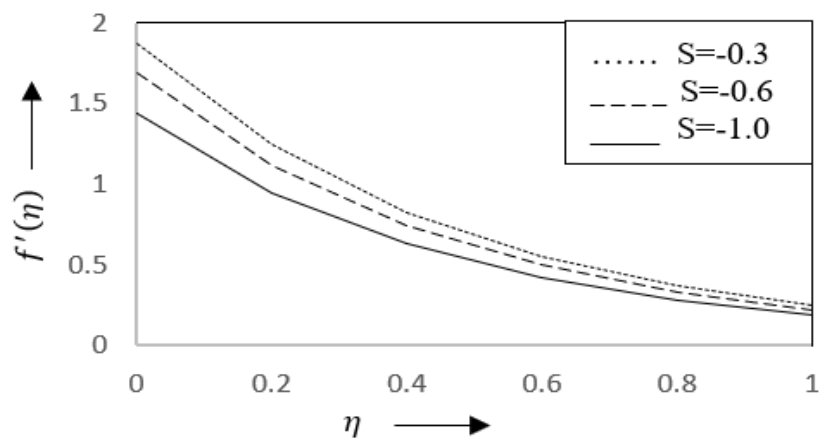


Fig. 4.5 Velocity profile $f'(\eta)$ against η for variation of S (blowing)

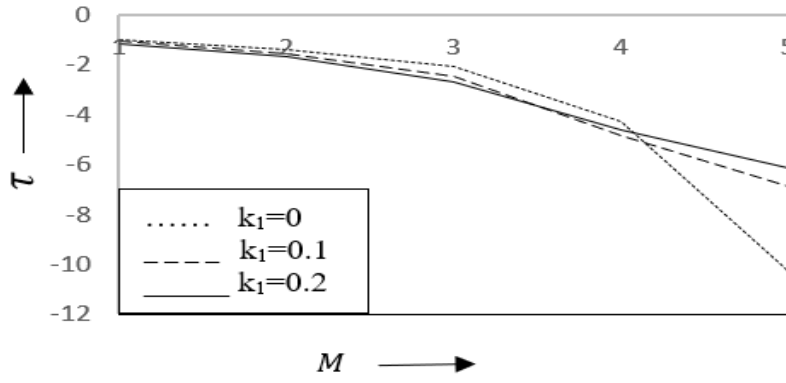


Fig. 4.6 Skin friction curves τ against M for variation of k_1

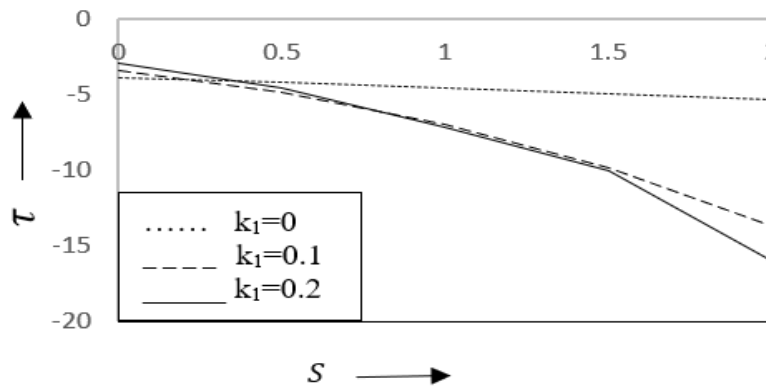


Fig. 4.7 Skin friction curves τ against S (suction) for variation of k_1

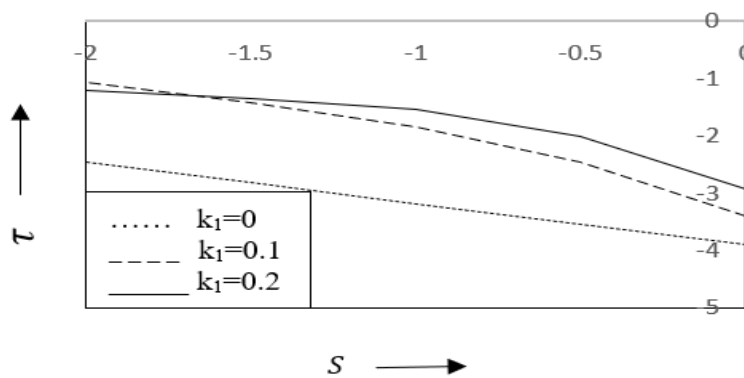


Fig. 4.8 Skin friction curves τ against S (blowing) for variation of k_1

4.5 Conclusion

The highly coupled nonlinear differential equations involved in this paper solved by homotopy perturbation technique. This method has advantage over the regular perturbation method. The effects of visco-elastic, magnetic and suction or blowing parameters on the velocity components and skin friction are investigated graphically. It is noticed that the flow field is significantly influenced by the elastic-viscous, magnetic and suction or blowing parameters. A future study investigating the flow simulation of the problem would be very interesting. Besides this, numerical method can also be implemented to find the solution of the same problem and the results obtained can be compared by analytical method. The flow simulation may give the clear picture of the problem.

The present study reveals the following important points:

- The fluid velocity reduces for elastico-viscous fluid as compared to Newtonian fluid ($k_1 = 0$).
- Setting $k_1 = 0$ provides all results corresponding to Newtonian fluid.
- The fluid velocity gradually reduces and ultimately vanishes with progressive distance for variations of elastico-viscous and magnetic parameters.
- The boundary layer thickness diminishes with the growth of magnetic parameter.
- The velocity profile enhances as applied suction rises whereas reverse pattern is observed for blowing.
- The boundary layer thickness reduces when blowing parameter acts on the flow field but suction acts oppositely